In-situ Fabrication of MoO_2-$Ni_3(PO_4)_2$/NF Heterojunction Composite Material for Application as Supercapacitor Electrode

Zhongxin Jin[a, b, 1]*, Feng Lin[a, 1], Caiying Li[a], Cheng Shao[a], Yang Xu[a], Fangze Li[a], Haijun Pang[b, *], Huiyuan Ma[b, *]

[a]Key Laboratory of Oilfield Applied Chemistry and Technology, College of Chemical Engineering, Daqing Normal University, Daqing 163712, P.R. China

[b]School of Materials Science and Chemical Engineering, Harbin University of Science and Technology, Harbin 150040, P.R. China.

*Corresponding author. Zhongxin Jin, *E-mail:* jzx1128@126.com, Tel./fax: +86-0451-86688575.

*Corresponding author. Haijun Pang, *E-mail:* panghj116@163.com, Tel./fax: +86-0451-86688575.

*Corresponding author. Huiyuan Ma, *E-mail:* mahy017@163.com, Tel./fax: +86-0451-86392716.

[1]These authors share co-first-authorship.

Content

1. Experimental Section

1.1. Reagents and Materials

Ammonium molybdate, Analytical pure, Tianjin Chemical Reagent Factory No. 4. Nickel sulfate hexahydrate, Analytical pure, Sinopharm Group Chemical Reagent Co., LTD. Ammonium persulfate, Analytically pure, Tianjin Zhiyuan Chemical Reagent Co., LTD. Urea, Analytical Pure, Liaoning Quanrui Reagent Co., LTD. Ammonium fluoride, Analytical pure, Liaoning Quanrui Reagent Co., LTD. Sodium hypophosphite, Analytical pure, Liaoning Quanrui Reagent Co., LTD. Nafion, Shanghai Aladdin Biochemical Reagent Co., LTD. Activated carbon, YP-50F, Kori Chemical Co., LTD. Acetylene black, Analytically pure, Tianjin Fuyu Fine Chemical Co., LTD. Polytetrafluoroethylene (PTFE), 60%, Aladdin. Nickel Foam (NF), conventional, Beijing Chemical Plant，Acetone, Analytical pure, Tianjin Fuyu Fine Chemical Co., LTD. Anhydrous ethanol, Analytical pure, Tianjin Tianli Chemical Reagent Co., LTD.

1.2. Synthesis of the Polyoxometalate Precursor $(NH_4)_6[NiMo_9O_{32}]\cdot 6H_2O$

First, 11.1204 g of $(NH_4)_6Mo_7O_{24}\cdot 4H_2O$ was weighed and dissolved in 100 mL of deionized water with stirring until fully dissolved. The pH of the solution was then adjusted to 4.44 using 2 mol/L H_2SO_4. Subsequently, 1.6074 g of nickel sulfate dissolved in 100 mL of water was added to the solution. The mixture was stirred and heated to a gentle boil. Following this, 1.3692 g of ammonium persulfate dissolved in 100 mL of water was poured into the solution. The heating was continued until the solution turned red, maintaining boiling with stirring for 1 hour. The solution was then left to stand overnight at room temperature, resulting in the precipitation of dark red crystals. The crystals were collected by vacuum filtration and dried at 60°C to obtain the dark red crystals of $(NH_4)_6[NiMo_9O_{32}]\cdot 6H_2O$ [1].

1.3. FT-IR Analysis of $(NH_4)_6[NiMo_9O_{32}]\cdot 6H_2O$

Fourier Transform Infrared Spectroscopy (FT-IR) was used to test the spectrum of $(NH_4)_6[NiMo_9O_{32}]\cdot 6H_2O$, and the test range was 4000~400 cm^{-1}. As can be seen from **Fig. S1**, the vibration peaks of 931 cm^{-1} and 894 cm^{-1} are the stretching vibration peaks

of Mo=O. The vibration peaks of 675 cm^{-1}, 600 cm^{-1}, and 545 cm^{-1} are generated by Mo-O-Mo bending vibration, and the vibration peak of 500 cm^{-1} are generated by Ni-O-Mo bending vibration. There is also a Ni-O stretching vibration peak at 714 cm^{-1} [2]. In addition, the vibration absorption peaks of NH_4^+ and H_2O are ν_{N-H}=3145 cm^{-1}, δ_{H-N-H}=1400 cm^{-1}, ν_{O-H}=3500 cm^{-1}, δ_{H-O-H}=1600 cm^{-1}.

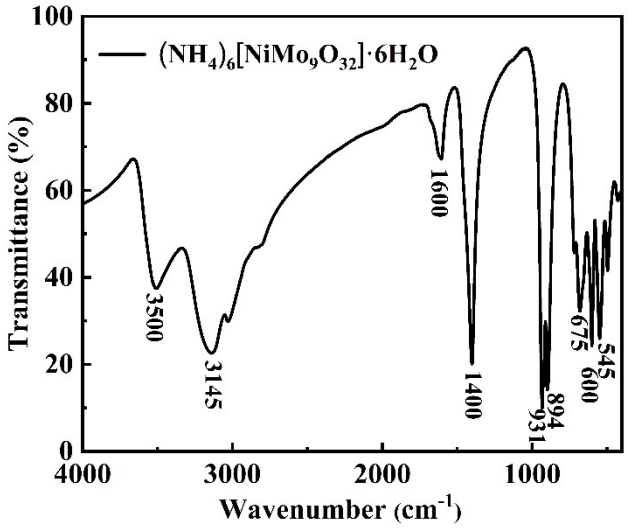

Fig. S1 FT-IR of $(NH_4)_6[NiMo_9O_{32}]\cdot 6H_2O$.

1.4. TGA Analysis of $(NH_4)_6[NiMo_9O_{32}]\cdot 6H_2O$

Fig. S2 shows the thermogravimetric analysis (TGA) curve of the polyoxometalate $(NH_4)_6[NiMo_9O_{32}]\cdot 6H_2O$ in a nitrogen atmosphere, heated at a rate of 5 ℃/min from 0 to 1200 ℃. The weight loss in the range of 0-460 ℃ is 13.84% (theoretical weight loss is 12.72%), corresponding to the loss of ammonia and crystallization water. In the range of 460-755 ℃, the structure is relatively stable. Beyond 755 ℃, a sharp decrease in mass indicates the collapse of the polyoxometalate framework. The weight loss between 755-1200 ℃ is 37.5% (theoretical value is 38.1%), corresponding to the loss of three structural water molecules and four sublimed MoO_3 molecules. The maximum weight loss rate occurs in the 755-950 ℃ range. At 1200 ℃, the residual mass is 48.9% (theoretical value is 49.1%), consisting of nickel and molybdenum oxides, specifically one NiO_2 and five MoO_3.

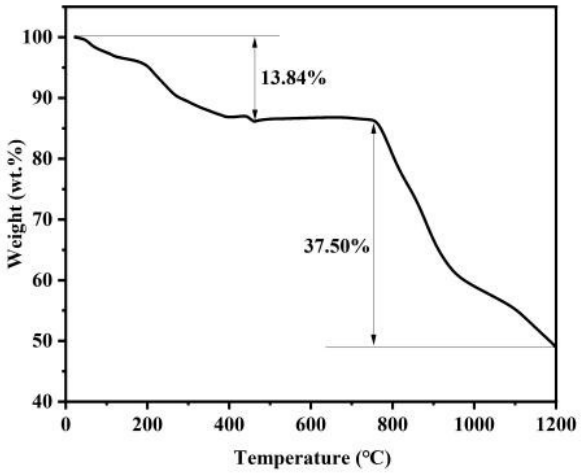

Fig. S2 TGA curves of $(NH_4)_6[NiMo_9O_{32}]\cdot 6H_2O$.

1.5. XRD Analysis of the $Ni(OH)_2$-$NiMoO_4$

Fig. S3 shows the XRD pattern of the powder after hydrothermal method. The diffraction peaks of the electrode material at 2θ = 11.64 ° and 39.06 ° match the standard PDF pattern ($3Ni(OH)_2$-$2H_2O$ PDF#22-0444), corresponding to the (001) and (200) crystal planes, respectively[3]. The diffraction peaks of the electrode material at 2θ = 16.12 °, 23.95 °, 28.80 °, 32.37 °, and 45.73 ° match the standard PDF pattern ($NiMoO_4$ PDF#33-0948), corresponding to the (011), (-121), (220), (130), and (141) crystal planes, respectively [4]. Therefore, the product is named $Ni(OH)_2$-$NiMoO_4$ composite.

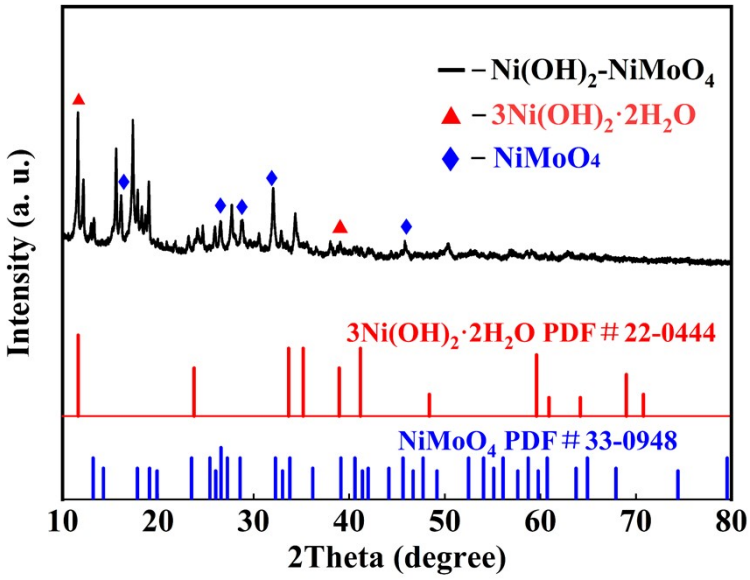

Fig. S3 XRD patterns of $Ni(OH)_2$-$NiMoO_4$ composite.

1.6. XPS Analysis of the MoO_2-$Ni_3(PO_4)_2$/NF

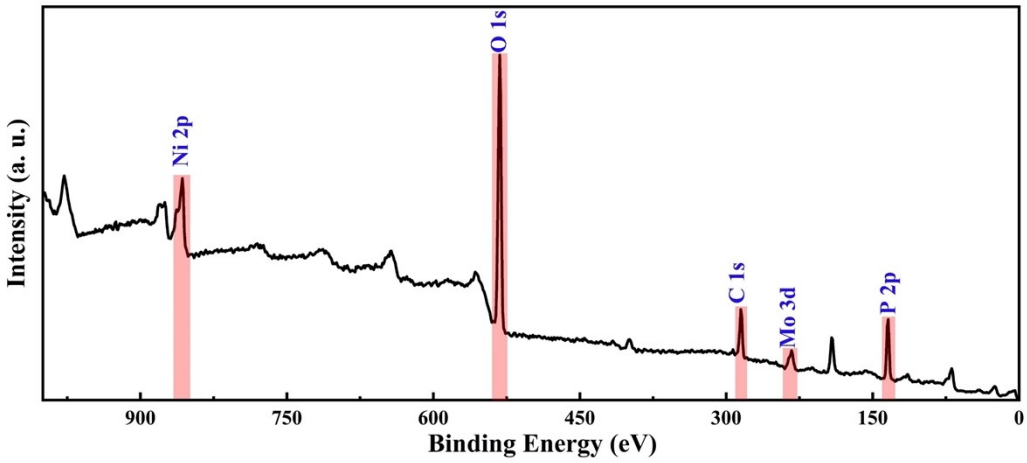

Fig. S4 The full-scan spectrum XPS spectrum of MoO_2-$Ni_3(PO_4)_2$/NF electrode materials.

1.7. Electrochemical impedance spectroscopy (EIS)

Fig. S5 shows the EIS with equivalent circuit model. The EIS data were fitted using the equivalent circuit model, Rs (Ω) and Rct (Ω) represent the solution resistance and charge transfer resistance, respectively [5].

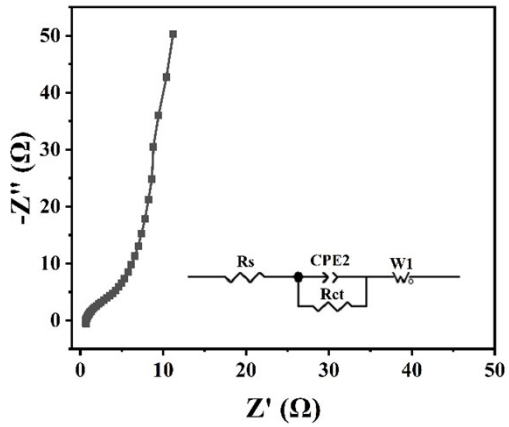

Fig. S5 EIS and equivalent circuit model of the MoO_2-$Ni_3(PO_4)_2$/NF.

Table S1 Fitting parameters for EIS data for all the samples.

Different electrode materials	Rs	Rct
MoO_2-$Ni_3(PO_4)_2$/NF-450℃-0.44g	0.506 Ω	19.07 Ω
MoO_2-$Ni_3(PO_4)_2$/NF-420℃-0.44g	0.622 Ω	23.55 Ω

MoO_2-$Ni_3(PO_4)_2$/NF-480℃-0.44g	0.634 Ω	26.61 Ω
MoO_2-$Ni_3(PO_4)_2$/NF-450℃-0.22g	0.559 Ω	32.64 Ω
MoO_2-$Ni_3(PO_4)_2$/NF-450℃-0.88g	0.555 Ω	26.87 Ω

1.8. Assembly and Characterization of Asymmetric Supercapacitors (ASC)

The formula for calculating the mass of the positive and negative electrode materials in asymmetric supercapacitor (ASC) devices is as follows [6]:

$$\frac{m_+}{m_-} = \frac{C_- \Delta V_-}{C_+ \Delta V_+} \quad (1)$$

Where the specific capacitance of the negative electrode of C_- is measured in $F \cdot g^{-1}$, the voltage window of negative electrode of ΔV_- is measured in V, the specific capacitance of the positive electrode of C_+ is measured in $F \cdot g^{-1}$, and the voltage window of the positive electrode of ΔV_+ is measured in V.

To evaluate the electrochemical performance of the electrode materials as the positive electrode in supercapacitors, the positive electrode materials were prepared with a composition of the MoO_2-$Ni_3(PO_4)_2$/NF (85 wt%), acetylene black (10 wt%), and PTFE (5 wt%). The negative electrode was prepared using activated carbon to substitute the MoO_2-$Ni_3(PO_4)_2$/NF. Both electrodes were subjected to cyclic voltammetry (CV) and galvanostatic charge-discharge (GCD) testing. The mass ratio of the negative to positive electrode materials in the assembled cell was calculated using Equation (1). With a total mass of 27.4 mg for the positive and negative electrodes, the electrodes for the cell were prepared using the same method as for the test electrodes. A separator, gasket, and spring were included, and the cell was assembled into a coin cell with 6 M KOH solution as the electrolyte. Two batteries were prepared in duplicate, which could light an LED bulb, as shown in **Fig. S6**.

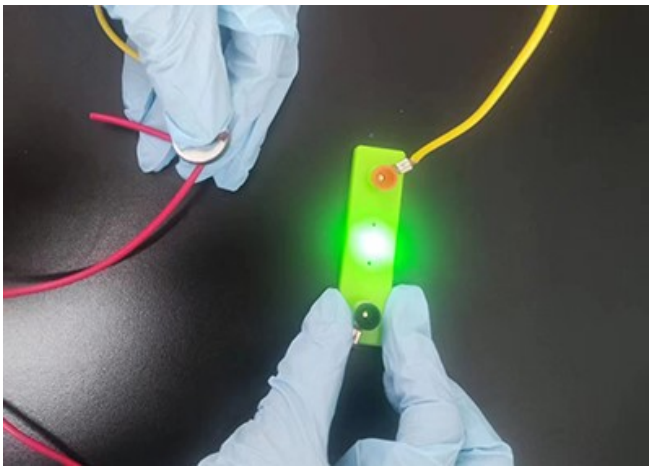

Fig. S6 The ASC device lights the bulb.

Table S2 A comparison of specific capacitance values and specific capacitance retention rates with previous literature.

Electrode materials	Specific capacitance	Stability cycle number	Reference
MoO_2-$Ni_3(PO_4)_2$/NF	396 $F \cdot g^{-1}$	82.2%	This work
$NiMoO_4$	392.53 $F \cdot g^{-1}$	87.14%	[7]
PPy/Go/ZnO	94.6 $F \cdot g^{-1}$	74%	[8]
PPy/gum arablk	368 $F \cdot g^{-1}$	85%	[9]
microporous carbon/ PANI	224 $F \cdot g^{-1}$	80%	[10]
mesoporous MoO_2	140 $F \cdot g^{-1}$	90%	[11]
N-doped graphene/Fe_3O_4	220 $F \cdot g^{-1}$	95%	[12]
Fe_3O_4/CNF (1D)	135 $F \cdot g^{-1}$	91%	[13]
MnO_2/BPC	139.6 $F \cdot g^{-1}$	92.3%	[14]
AL-Co/ NGC-800	56.6 $F \cdot g^{-1}$	90.6%	[15]

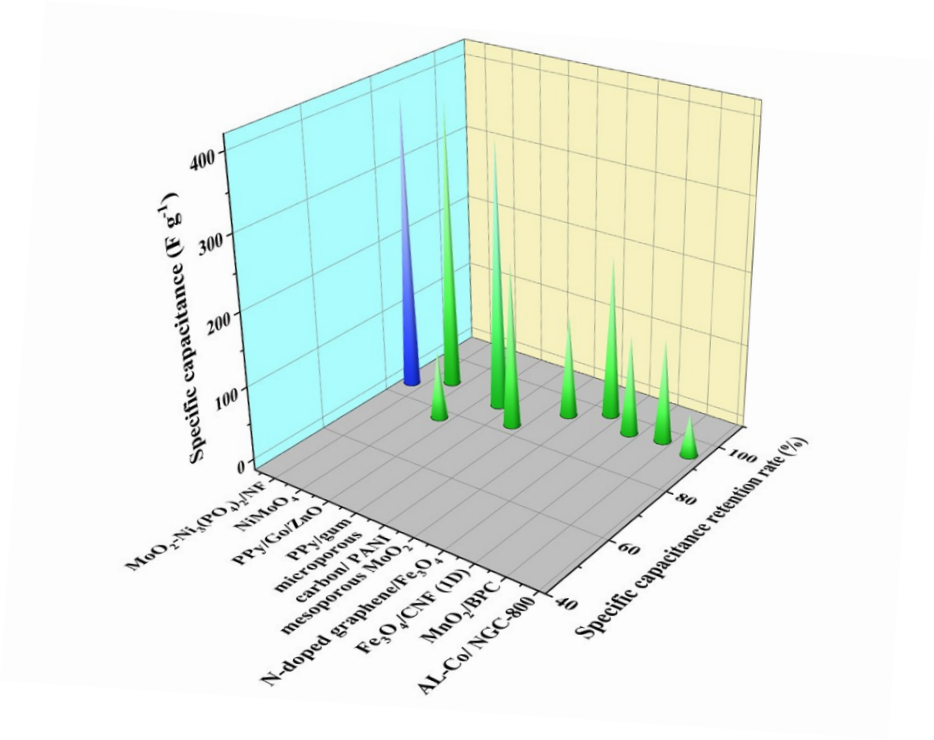

Fig. S7 A comparison graph of specific capacitance values and specific capacitance retention rates.

Table S3 The mass loading of the electrode material.

Electrode material	$\triangle m$
MoO_2-$Ni_3(PO_4)_2$/NF-450℃-0.22g	0.0020 g
MoO_2-$Ni_3(PO_4)_2$/NF-450℃-0.44g	0.0018 g
MoO_2-$Ni_3(PO_4)_2$/NF-450℃-0.88g	0.0013 g
MoO_2-$Ni_3(PO_4)_2$/NF-420℃-0.44g	0.0015 g
MoO_2-$Ni_3(PO_4)_2$/NF-480℃-0.44g	0.0012 g

References

[1] E. Ni, S. Uematsu, T. Tsukada and N. Sonoyama, *Solid State Ion.*, 2016, **285**, 83-90.

[2] S. J. Dunne, R. C. Burns and G. A. Lawrance, *Aust. J. Chem.*, 1992, **45**, 1943-1952.

[3] J. Yan, Z. Fan, W. Sun, G. Ning, T. Wei, Q. Zhang, R. Zhang, L. Zhi and F. Wei, *Adv. Funct. Mater.*, 2012, **22**, 2632-2641.

[4] D. Cai, D. Wang, B. Liu, Y. Wang, Y. Liu, L. Wang, H. Li, H. Huang, Q. Li and T.

Wang, *ACS Appl. Mater. Inter.*, 2013, **5**, 12905-12910.

[5] B. S. Chikkatti, A. M. Sajjan, N. R. Banapurmath, J. K. Bhutto, R. Verma and T. M. Yunus Khan, *Polymer-Basel.*, 2023, **15**, 4587.

[6] D. C. Martínez-Casillas, I. L. Alonso-Lemus, I. Mascorro-Gutiérrez and A. K. Cuentas-Gallegos, *J. Electrochem. Soc.*, 2018, **165**, A2061.

[7] P. Sharma, M. Minakshi, J. Whale, A. Jean-Fulcrand and G. Garnweitner, *Nanomaterials*, 2021, **11**, 580.

[8] W. K. Chee, H. N. Lim, I. Harrison, K. F. Chong, Z. Zainal, C. H. Ng and N. M. Huang, *Electroc. Acta*, 2015, **157**, 88-94.

[9] R. Ullah, N. Khan, R. Khattak, M. Khan, M. S. Khan and O. M. Ali, *Polymers*, 2022, **14**, 242.

[10] A. V. Sosunov, M. Rajapakse, G. A. Rudakov, R. S. Ponomarev, V. K. Henner, J. B. Jasinski, D. A. Buchberger, M. S. Reza, B. Karki, G. Sumanasekera, *Surf. Eng. Appl. Electrochem.*, 2022, **58**, 87-93.

[11] X. Li, J. Shao, J. Li, L. Zhang, Q. Qu and H. Zheng, *J. Power Sources*, 2013, **237**, 80-83.

[12] L. Li, Y. Dou, L. Wang, M. Luo and J. Liang, *RSC Adv.*, 2014, **4**, 25658-25665.

[13] J. Mu, B. Chen, Z. Guo, M. Zhang, Z. Zhang, P. Zhang, C. Shao and Y. Liu, *Nanoscale*, 2011, **3**, 5034-5040.

[14] G. Yang, S. J. Park, *J. Alloys Compd.*, 2018, **741**, 360-367.

[15] S. R. Mane, S. Pradhan, V. Somkuwar, R. Bhattacharyya, P. C. Ghosh and N. Jha, *React Chem. Eng.*, 2023, **8**, 891-907.